Elastic constants of argon single crystals determined by Brillouin scattering*

S. Gewurtz† and B. P. Stoicheff
Department of Physics, University of Toronto, Toronto, Canada
(Received 9 May 1974)

Single crystals of argon were grown and investigated at 82.3 K, near the triple point. X-ray diffraction photographs taken in transmission were used to verify that the crystals were single and to determine their orientation. Brillouin spectra were obtained for several different orientations of three crystals. The observed spectra contained the longitudinal component and at least one, and sometimes both transverse components. Their frequency shifts were used to determine the adiabatic elastic constants at 82.3 K: $C_{11} = 2.38 \pm 0.04$, $C_{12} = 1.56 \pm 0.03$, $C_{44} = 1.12 \pm 0.03$, in units 10^{10} dyn/cm^2, and the elastic anisotropy $A = 2.73 \pm 0.10$. These values differ significantly from earlier results derived from neutron scattering and ultrasonic experiments. However, there is good agreement with recent Monte Carlo calculations which use multiparameter pair potentials and the triple-dipole interaction.

I. INTRODUCTION

Argon is the most thoroughly investigated of the rare-gas solids, both experimentally and theoretically. After the development of techniques for growing single crystals, by Simmons and his coworkers,[1] measurements of many of the bulk and thermal properties have been reported,[2] and the resulting values have been used to test available theories. Recently, there has also been some success in the derivation of interatomic potentials for argon: Parson, Siska, and Lee[3] have obtained a multiparameter pair potential which is in good agreement with the spectroscopic data of Tanaka and Yoshino[4] on diatomic argon, and with the molecular-beam studies of Scoles[5] and Lee[3] and their co-workers; Barker[6] and his colleagues have put forward other multiparameter pair potentials which are in good agreement with many of the properties of condensed argon. These recent determinations of interatomic potentials provide new incentives for further accurate experiments on argon.

One of the sensitive tests of theories of lattice dynamics, and of proposed interatomic potentials, is the comparison of computed values of the elastic constants with the observed values. Several determinations of the elastic constants of solid argon have been made from measurements of sound velocities obtained in neutron scattering and ultrasonic experiments. The most extensive and probably most accurate ultrasonic measurements on argon are those reported recently by Keeler and Batchelder.[7] However, their results are not compatible with those of two earlier ultrasonic experiments.[8,9] Similarly, the results of two recent investigations of neutron scattering, by Batchelder *et al.*[10] and Egger *et al.*,[11] are not in agreement with each other, and differ from the ultrasonic values by more than the quoted experimental errors. Finally, none of these experimental values agrees with the latest theoretical predictions.[12–14] The major difficulty in the ultrasonic and neutron scattering experiments seems to have been the requirement of large (~1 cm^3) single crystals; large crystals are difficult to grow and maintain, especially when bonded to transducers for the ultrasonic experiments.

The present investigation was initiated in the hope of resolving the conflicting experimental data on the elastic constants of argon. Recent experiments in this laboratory,[15,16] leading to the evaluation of the elastic constants of xenon and neon, have shown that Brillouin spectroscopy has distinct advantages over ultrasonic and neutron scattering techniques for investigating the elastic properties of the rare-gas solids. The most important advantage is that the size of the single crystal need only be approximately 1 mm^3: Such a small single crystal can be readily grown; also, it is transparent to x rays, thereby making it possible to demonstrate that the crystal is single and to determine its orientation accurately.

In the present experiment three different single crystals were investigated near the triple point of argon ($T = 83.81$ K and $P = 516.9$ Torr). This temperature was chosen since it is easiest to grow rare-gas single crystals near the freezing point; moreover, this is a most interesting temperature region since effects of anharmonicity are largest at this temperature. The crystals were grown from the liquid and maintained at 82.3 K in a specially designed Dewar cooled by liquid nitrogen. The quality of each crystal and its orientation were determined by Laue x-ray diffraction in transmission. Brillouin spectra were recorded for a large number of orientations of each crystal. The frequency shifts of the observed Brillouin components were used to obtain values of the adiabatic elastic constants C_{11}, C_{12}, C_{44} to an accuracy of 2.5% or better. The experimental method is described in detail in Sec. III. This is followed by a review of the observed

spectra and the results of their analyses in Sec. IV. Finally a comparison with existing data on the elastic properties of solid argon and with the results of current theories is given in Sec. V.

II. BRIEF RESUME OF BRILLOUIN SCATTERING IN CUBIC CRYSTALS

The theory of Brillouin scattering in cubic crystals has been discussed fully by Benedek and Fritsch, [17] and modified by Gornall and Stoicheff[15] to describe the scattering from a crystal having arbitrary orientation with respect to the incident light beam. Here, only the relevant equations will be repeated for ready reference.

It is well known that the fluctuations in the dielectric constant of a medium, $\delta\epsilon(\vec{r}, t)$, give rise to scattering of light. For a crystalline medium these fluctuations are written in terms of their spatial Fourier components as

$$\delta\epsilon(\vec{r}, t)=\left(\frac{1}{2\pi}\right)^{3/2}\sum_{\mu}\int |d\vec{q}|\,\delta\epsilon^{\mu}(\vec{q}, t)e^{i\vec{q}\cdot\vec{r}} \quad .$$

For a monatomic cubic crystal, there are three acoustic branches, one longitudinal and two transverse, associated with a wave vector $\vec{q}$, and these are denoted by the polarization index μ (where $\mu = 1, 2, 3$). The dispersion relation for these branches is

$$\omega_{\mu}(\vec{q}) = v_{\mu}(\vec{q})q ,$$

where ω_{μ} is the frequency and $v_{\mu}(\vec{q})$ is the velocity of the acoustic mode μ. In a light scattering experiment, the wave vector $\vec{q}$ is defined in the laboratory reference frame as $\vec{q}=\vec{k}-\vec{k}_0$ (where $\vec{k}_0$ and $\vec{k}$ are the wave vectors of the incident and scattered light), and its magnitude is given by

$$q = 2k_0\sin(\theta/2) ,$$

where θ is the scattering angle. The Brillouin frequency shift of a mode μ is

$$\Delta\nu_{\mu} = \pm(2\pi)^{-1}\omega_{\mu}(\vec{q}) = \pm 2\nu_0 v_{\mu}(\vec{q})(n/c)\sin(\theta/2), \quad (1)$$

where c is the velocity of light and n the refractive index.

Fluctuations in the dielectric constant arise from the coupling of propagating elastic waves to the dielectric tensor through the elasto-optic constants of the crystal. The propagation of these elastic waves in a crystal for which the stress tensor σ_{ij} and strain tensor obey Hooke's law is described by

$$\rho\ddot{u}_i = \frac{\partial\sigma_{ij}}{\partial r_j} ,$$

where $\vec{u}$ and $\vec{r}$ are the displacement and position vectors of an element of the crystal, and ρ is its density. For a monochromatic plane-wave solution of the form $\vec{u}=\vec{\Pi}(\vec{q})e^{i(\vec{q}\cdot\vec{r}-\omega t)}$ this system of equations may be written in the form

$$(\lambda_{ij}-\rho\omega^2\delta_{ij})\Pi_j = 0, \quad (2)$$

with

$$\lambda_{ij} = (C_{11}-C_{44})q_i^2 + C_{44}q^2 \quad \text{for } i=j$$
$$= (C_{12}+C_{44})q_iq_j \quad \text{for } i\neq j .$$

Here C_{11}, C_{12}, C_{44} are the elastic constants for a cubic crystal, and Π_1, Π_2, Π_3 are the components of the polarization vector in the direction of the displacement $\vec{u}$. The secular equation

$$|\lambda_{ij}-\rho\omega^2\delta_{ij}| = 0 \quad (3)$$

provides a relationship between the three elastic constants and the three mode frequencies $\omega = \pm\omega_{\mu}(\vec{q})$. This equation is most easily solved for $\vec{q}$ along crystal directions of high symmetry; for directions of low symmetry, Eq. (2) must be solved as a 3×3 eigenvalue problem. An orthogonal transformation is found which diagonalizes the matrix (λ_{ij}); the eigenvalues yield ω_{μ}, and the eigenfunctions yield Π_{μ}. Thus when the elastic constants are known, the frequencies can be determined directly, and if values of the elastic constants are assumed, values of ω_{μ} may be obtained for comparison with the experimental measurements.

III. EXPERIMENTAL APPARATUS AND TECHNIQUE

The apparatus and techniques used in the present experiment are essentially the same as those described by Gornall and Stoicheff[15] for the investigation of xenon. Therefore, only those features which are significantly different will be discussed below. As in the earlier work, single crystals of small dimensions (~2 mm diam and 1 cm long) were grown near the freezing point; they were examined by x-ray diffraction in transmission to ensure that they were single and to determine their orientation; and Brillouin spectra were recorded at high resolution for various crystal orientations, all at a scattering angle of 90° to the incident laser beam.

A. Cryostat and sample cell

A schematic diagram of the complete experiment is shown in Fig. 1, and a detailed drawing of the sample cell and cryostat tail assembly in Fig. 2. Since argon liquefies at 87.3 K and solidifies at 83.8 K (under its own vapor pressure) it was possible to use liquid N_2 cooling in this experiment. The cryostat consisted of a 5.5-liter reservoir for liquid N_2, and a rigid tail section consisting of a hollow copper block kept full of liquid N_2 by means of two hollow posts connected to the bottom of the reservoir. A cylindrical sample cell was mounted within this block, as described below, along with heaters and thermocouples for temperature control of the sample volume. The whole tail assembly was

enclosed in a removable Pyrex envelope fitted with an optical quality window at the bottom for laser irradiation of the sample, and a curved Mylar window (0.025 mm thick) cemented to the cylindrical surface for x-ray irradiation of the sample at right angles to the laser beam. The sample cell was carefully mounted so that its vertical axis coincided with that of the cryostat, and provision was made for rotating the complete cryostat about this axis.

The sample cell was constructed of Pyrex tubing of 2.0-mm bore, 0.5-mm wall, and ~5-cm length. A good quality window for the incident laser beam was made by polishing the upper end of a Pyrex rod (2.0 mm diam) fusing this into the bottom end of the cell and finally polishing the end. The top end of the cell was terminated in a horn (painted black) which served as a light trap. A 1-liter flask containing argon gas with natural isotopic abundance (research grade of nominal 99.9995% purity) and supplied by the Matheson Co. was connected to the sample cell as shown.

The cell was mounted within the copper block by means of two sleeves of thin copper, one cemented around the bottom window, and the other at the upper end of the cell, leaving a clear section of glass ~1 cm long between the sleeves. The other ends of the sleeves were cemented to the copper block. A cylinder of thin copper, having appropriate apertures for the scattered light and x rays, was attached to the bottom sleeve and served as a heat shield. Good thermal coupling of the cell and coolant was thus provided so that a temperature as low as 79 K was readily attained within the cell.

Long-term temperature control was essential in this experiment since the process of growing a single crystal, the determination of its quality and orientation, and the subsequent scattering experiments often took two to four weeks. This was achieved with the heaters and thermocouples shown in Fig. 2 using the method described in the xenon work. With the cell kept at a temperature of 85.5

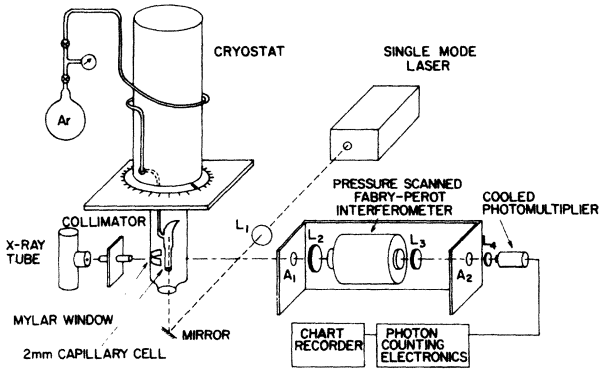

FIG. 1. Schematic diagram of apparatus for Brillouin scattering and x-ray diffraction of argon single crystals.

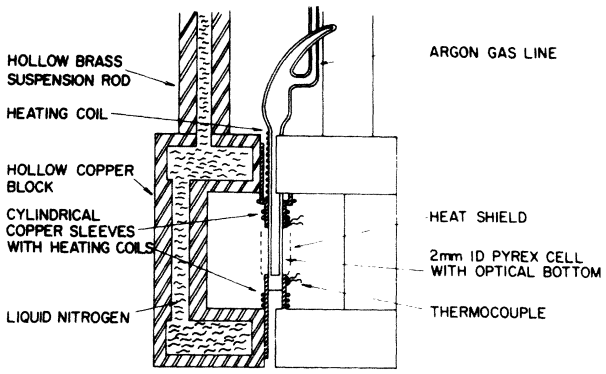

FIG. 2. Schematic diagram of tail assembly showing details of sample cell, cooling system, and temperature control.

K, argon gas was admitted to the cell until it was full of liquid. A small "seed" crystal (dimensions < 1 mm) was then grown by slowly lowering the temperature of the bottom of the cell until a 2° temperature gradient was established in the cell. This seed crystal was annealed for ~12 h; the temperature of the bottom end was then slowly lowered causing the crystal to grow to a height of ~1 mm. After a second annealing for several hours, the temperature of the top of the cell was lowered (at a rate of ~1°/h) until the crystal filled the cell. At this stage the temperature gradient from top to bottom of the cell was 3.3°, with the center at a temperature of 82.3 K.

B. X-ray diffraction

X-ray diffraction was used to ensure that the crystals were single and to determine each orientation in the laboratory reference frame. Transmission Laue patterns were used since they probe the full cross section of the crystal. The x-ray beam from a tungsten target was collimated to give a 2-mm-diam beam at the sample. Diffraction photographs were taken at a distance of 6.80 cm from the center of the sample on Polaroid type 57 film held in a Polaroid XR-7 cassette equipped with a fluorescent backing. Photographs were taken before and after each Brillouin spectrum. Exposure times of 10 min were sufficient to produce ~10 distinct Laue spots, but longer exposures were used at each orientation to ensure accurate measurement and identification of even the weakest Laue spots.

A Laue photograph for one orientation is reproduced in Fig. 3, showing a typical arrangement of Laue spots in a closed ellipse passing through the center of the photograph. This pattern is caused by reflections from lattice planes belonging to the same crystal zone, and facilitates the analysis of the crystal orientation. A preliminary graphical

analysis yielded values of the Euler angles (θ, ϕ, χ) accurate to ~2°. This was followed by an accurate measurement (to 0.5 mm) of the coordinates of each Laue spot and a computation of a series of complete diffraction patterns for a small range of Euler angles about their preliminary values. The most reliable Euler angles were then determined by a least-squares fit of the coordinates, and the corresponding Laue pattern given by the IBM 7094 Calcomp plotter was matched to the x-ray photograph. In this way, the Euler angles for each orientation were determined to an accuracy of 0.5°.

A crystal was judged to be single when every observed Laue spot on a given photograph was reproduced on the corresponding calculated pattern, and when this criterion was satisfied for all crystal orientations.

C. Brillouin scattering

A He-Ne laser was used in the preliminary experiments with crystal No. 1. It was built according to the design of Smith.[18] It emitted 10 mW of radiation at 6328.2 Å, in a single mode, and was stabilized in frequency and intensity. The experiments with crystals 2 and 3 were carried out with a Spectra Physics (model 165) Ar^+ laser using a tilted etalon. Radiation at 4879.9 Å was emitted in a single mode having a short-term frequency jitter of ±10 MHz and a slow frequency drift < 50 MHz/h. The laser power incident on the crystals was ~6 mW in these experiments, and was constant to 0.5%. The advantages of the Ar^+ radiation for Brillouin scattering were the higher scattering power, and the higher sensitivity of the photomultiplier (with S-20 spectral response) to radiation at 4880 Å.

The laser radiation was directed along the vertical axis of the cell and focused in the crystal. Light scattered at 90° ±0.5° to the incident beam was collected and examined with the Fabry-Perot spectrometer illustrated in Fig. 1, and described in Ref. 15. Care was taken in the alignment to ensure that the scattered light collected by this optical system originated within the volume of the crystal sampled by the x-ray beam. In the present experiments, two interferometers were used, one for 6328-Å radiation, the second for 4880-Å radiation. The respective spacers were 0.9993 ± 0.0002 and 1.0030 ± 0.0002 cm giving spectral-free ranges of 0.4999 (14 996) and 0.4980 cm^{-1} (14 940 MHz). The interferometer plates were flat to $\lambda/200$ and dielectrically coated to give 98% reflectivity. A finesse of 100 to 120 was achieved in each recorded spectrum, resulting in an instrumental width of ~150 MHz. The photomultiplier dark counting rate was ~1 per second. Brillouin spectra were recorded at a speed of 1 spectral-free range every 45 min, and 3 to 5 orders constituted a complete scan for each orientation of the crystal.

IV. EXPERIMENTAL RESULTS

A. Observed Brillouin spectra

Three single crystals of argon were grown for this investigation. Preliminary experiments were carried out with crystal 1 using 6328-Å radiation;

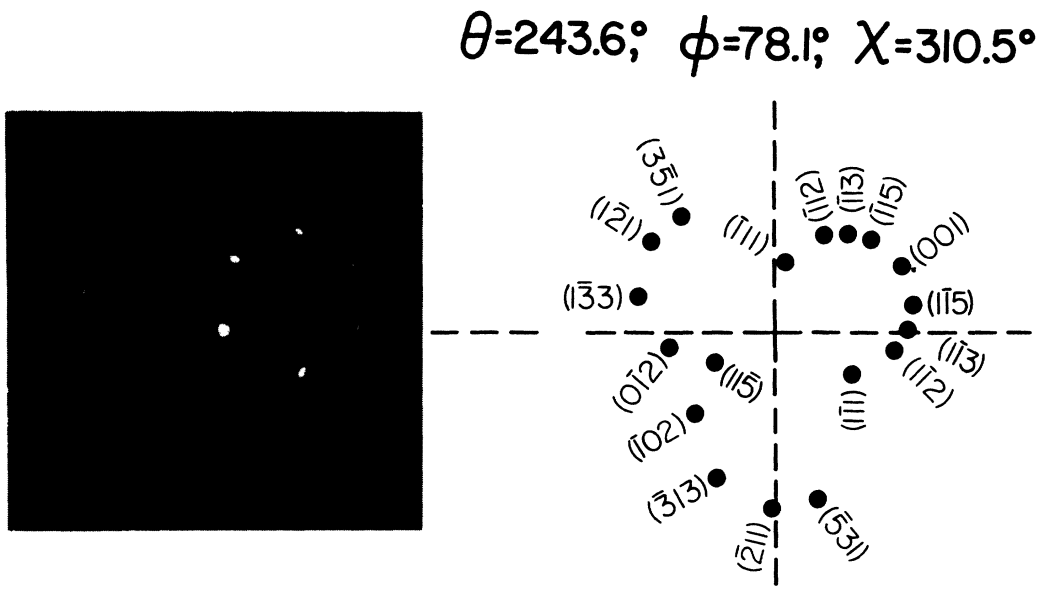

FIG. 3. Photograph of Laue diffraction pattern of crystal 3 ($\theta = 243.6°$, $\phi = 78.1°$, $\chi = 310.5°$) and the computed pattern which identified the crystal orientation. The solid circles in the computed pattern correspond to the observed diffraction spots.

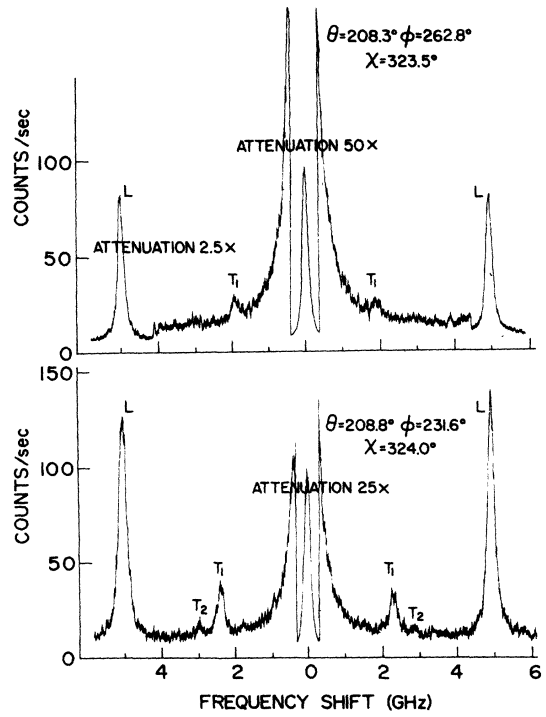

FIG. 4. Brillouin spectra of crystal 2 showing the variation in intensity with crystal orientation.

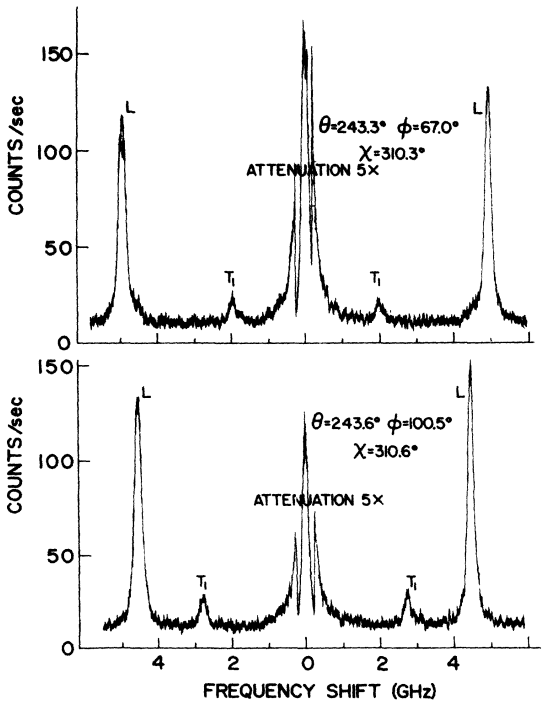

FIG. 5. Brillouin spectra of crystal 3 showing the variation in frequency shift with crystal orientation.

more extensive experiments were carried out on crystals 2 and 3 using 4880-Å radiation. The crystals did not appear to grow preferentially along the cell axis: In fact, the inclinations of the primitive cell axes [100], [010], [001] to the vertical cell axis were 50.4°, 52.1°, and 62.3° for crystal 1; 73.7°, 67.8°, and 28.1° for crystal 2; 46.8°, 54.8°, and 63.5° for crystal 3.

Brillouin spectra for crystal 1 were recorded at eight different orientations with the Euler angle ϕ varied over a range of ~55°; for crystal 2, spectra at 12 orientations over a range of 90° in ϕ; and for crystal 3, spectra at nine orientations over a range of 95° in ϕ. Typical Brillouin spectra are shown in Figs. 4 and 5, and the measured frequency shifts are given in Table I. Most of the observed spectra consisted of two Brillouin components, the longitudinal and the low-frequency transverse components. Only for three orientations of crystal 2 were all three components observed, and even in these spectra the high-frequency transverse component (labeled T_2) was of very low intensity (Fig. 4). It is evident from the spectra in Fig. 5 that the fre-

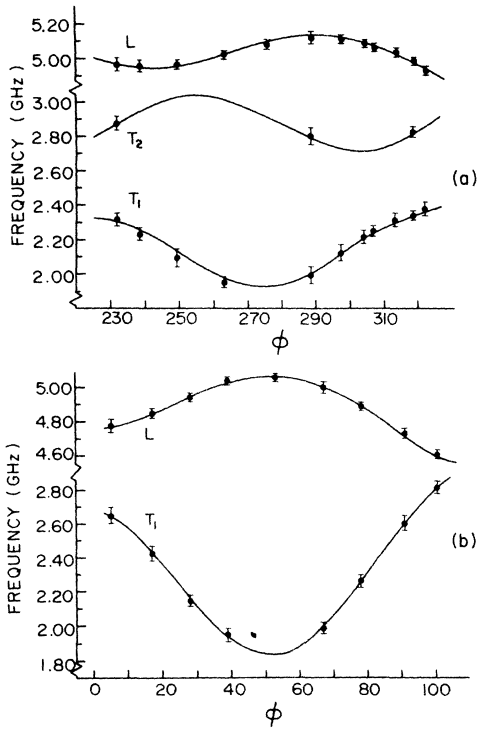

FIG. 6. Graphs of acoustic-mode frequencies as a function of orientation angle ϕ: (a) crystal 2, and (b) crystal 3. The indicated errors on the experimental points include inaccuracies in measurements of orientation angles as well as of frequency shifts. The solid lines represent the "best fit" used to determine values of the elastic constants.

TABLE I. Experimental Brillouin shifts.[a] $T = 82.3$ K; $P = 482$ Torr.[b]

Euler angles (deg)			Frequency shifts		
θ	ϕ	χ	L	T_1	T_2
			Crystal No. 1		
297.4	219.3	313.7	3.860 ± 0.019	...	...
297.9	229.1	313.9	3.895 ± 0.012	...	...
297.7	239.6	313.9	3.905 ± 0.015	...	...
297.5	249.3	313.7	3.850 ± 0.014	1.572 ± 0.016	...
297.8	259.3	313.7	3.764 ± 0.015	1.761 ± 0.006	...
297.7	264.4	313.4	3.741 ± 0.022	1.881 ± 0.020	...
297.7	269.5	313.7	3.665 ± 0.014	1.978 ± 0.013	...
297.7	274.4	313.7	3.603 ± 0.012	2.085 ± 0.015	...
			Crystal No. 2		
208.8	231.6	324.0	4.964 ± 0.025	2.315 ± 0.022	2.876 ± 0.024
208.5	238.3	324.0	4.956 ± 0.025	2.231 ± 0.019	...
208.7	249.1	323.9	4.966 ± 0.014	2.093 ± 0.037	...
208.3	262.8	323.5	5.022 ± 0.015	1.957 ± 0.019	...
208.6	275.4	323.4	5.084 ± 0.015	...	...
208.1	288.3	323.5	5.127 ± 0.031	1.997 ± 0.033	2.804 ± 0.031
208.5	297.1	323.2	5.120 ± 0.018	2.126 ± 0.028	...
208.5	303.9	323.1	5.093 ± 0.014	2.219 ± 0.025	...
208.4	306.9	323.2	5.070 ± 0.015	2.253 ± 0.023	...
208.0	313.0	323.8	5.042 ± 0.021	2.318 ± 0.028	...
207.8	318.4	323.9	4.995 ± 0.012	2.345 ± 0.014	2.833 ± 0.023
208.5	321.8	322.8	4.937 ± 0.020	2.385 ± 0.021	...
			Crystal No. 3		
243.5	5.0	309.7	4.776 ± 0.025	2.648 ± 0.026	...
243.5	16.9	309.9	4.847 ± 0.014	2.422 ± 0.016	...
243.5	28.0	310.1	4.942 ± 0.019	2.144 ± 0.007	...
243.5	39.0	310.2	5.041 ± 0.011	1.951 ± 0.018	...
243.5	53.0	310.3	5.065 ± 0.012	...	...
243.3	67.0	310.3	5.008 ± 0.022	1.989 ± 0.017	...
243.6	78.1	310.5	4.898 ± 0.011	2.267 ± 0.012	...
243.0	91.0	310.6	4.740 ± 0.017	2.607 ± 0.015	...
243.6	100.5	310.6	4.617 ± 0.017	2.820 ± 0.017	...

[a]Average values of at least six measurements for which the average deviation is given.
[b]The equilibrium vapor pressure corresponding to 82.3 K is 415 Torr; the measured pressure given here is somewhat higher because each crystal was maintained with a temperature gradient.

quency shifts of the Brillouin components changed significantly with crystal orientation. This dependence of frequency shift on crystal orientation is shown more completely for crystals 2 and 3 in Fig. 6. Each of the frequency shifts listed in Table I is an average of at least six measurements, and the accuracy is estimated to be better than 1%.

The peak intensities of all of the observed Brillouin components were measured, and the ratios of transverse to longitudinal intensities are listed in Table II and plotted vs orientation angle in Fig. 7. Measurements of the peak intensities were made rather than integrated intensities since all of the observed linewidths were the same (and equal to the instrumental width). Each value in Table II is the average of at least six measured ratios. The average deviations for $I(T_1)/I(L)$ range from 5 to 12%. Because of the very low intensity of the T_2 component in the three spectra in which it was observed, the accuracy of $I(T_2)/I(L)$ was ~25% at best.

B. Evaluation of elastic constants

In none of the orientations for which spectra were recorded was the wave vector $\vec{q}$ aligned with a major symmetry direction of the crystal. Thus, the elastic constants could not be determined from Eq. (3) as explicit functions of the acoustic-mode frequencies. Furthermore, the problem was complicated by the fact that in all but three of the observed Brillouin spectra the transverse component T_2 could not be detected.

The elastic constants were evaluated using the method described in Ref. 15. Trial values of C_{11}, C_{12}, and C_{44} were substituted into the dynamical equations, Eq. (2), and the frequencies of the longitudinal mode L and the lower-frequency transverse mode T_1 were obtained by solving the eigenvalue problem as outlined in Sec. II. For a given

TABLE II. Experimental peak intensity ratios[a] as a function of crystal orientation.

ϕ (deg)	$I(L)/I(T_1)$	$I(L)/I(T_2)$
	Crystal No. 2	
231.6	0.186 ± 0.023	0.041 ± 0.011
238.3	0.166 ± 0.015	• • •
249.1	0.121 ± 0.018	• • •
262.8	0.048 ± 0.009	• • •
288.3	0.040 ± 0.010	0.029 ± 0.006
297.1	0.113 ± 0.010	• • •
303.9	0.136 ± 0.010	• • •
306.9	0.156 ± 0.008	• • •
313.0	0.155 ± 0.009	• • •
318.4	0.151 ± 0.009	0.020 ± 0.009
321.8	0.140 ± 0.006	• • •
	Crystal No. 3	
5.0	0.207 ± 0.017	• • •
16.9	0.226 ± 0.012	• • •
28.0	0.179 ± 0.016	• • •
39.0	0.089 ± 0.007	• • •
67.0	0.103 ± 0.011	• • •
78.1	0.178 ± 0.016	• • •
91.0	0.172 ± 0.019	• • •
100.5	0.132 ± 0.012	• • •

[a]Average values of at least six measurements for which the average deviation is given.

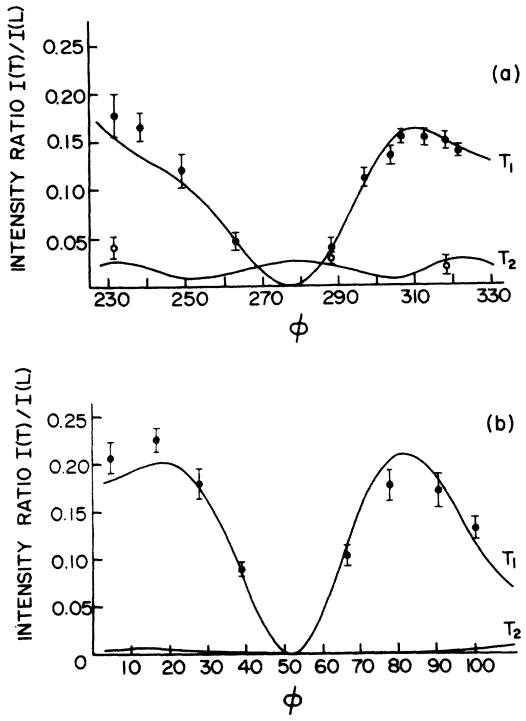

FIG. 7. Graphs of the intensity ratios $I(T_1)/I(L)$ and $I(T_2)/I(L)$ of the Brillouin components in the spectra of: (a) crystal 2, and (b) crystal 3. The solid lines represent the "best fit" used to determine the ratios of the photoelastic constants.

set of elastic-constant values, the frequencies of the L and T_1 acoustic modes were obtained for all orientations of the crystal at which spectra were taken. The trial values of the acoustic-mode frequencies were compared to the corresponding experimental frequency shifts and a fit was obtained for each crystal by the method of least squares. In Figs. 6(a) and 6(b), the experimental Brillouin shifts observed in crystals 2 and 3 are shown plotted as a function of ϕ. The solid curves in these figures represent solutions of the dynamical equations which best fit all of the experimental frequency shifts of the L and T_1 Brillouin components. Although the frequency shift of the T_2 component of crystal 2 was not included in the fit of Fig. 6(a), good agreement with the predicted curve of T_2 is seen for those orientations where this mode was detected. The values of the elastic constants determined in this way are given in Table III and labeled (all ϕ).

A second method of analysis was used for those orientations of crystal 2 for which all three Brillouin frequency shifts could be measured, namely, $\phi = 231.6°$, $288.3°$, and $318.4°$. In this analysis, an independent determination of the three elastic constants was made for each orientation from the L, T_1, and T_2 Brillouin shifts. Again, the method involved trying various values of the elastic constants in Eq. (2) and finding the best agreement with the experimental frequency shifts. The elastic constants determined by this analysis are also given in Table III. However, it should be emphasized that these values of C_{11}, C_{12}, and C_{44} are not of high accuracy because the observed T_2 components were extremely weak in all three spectra and their frequency shifts were difficult to measure.

Since the three crystals were maintained at the same temperature and pressure it is of interest to determine the values of the elastic constants which

TABLE III. Adiabatic elastic constants of argon, [$T = 82.3$ K],[a] determined from the Brillouin spectra.

Crystal No.	Elastic constants (10^{10} dyn/cm^2) C_{11}	C_{12}	C_{44}
1 (all ϕ)	2.33 ± 0.08	1.49 ± 0.06	1.17 ± 0.07
2 (all ϕ)	2.38 ± 0.06	1.55 ± 0.05	1.11 ± 0.05
3 (all ϕ)	2.38 ± 0.04	1.57 ± 0.03	1.12 ± 0.03
2 ($\phi = 231.6°$)	2.34	1.54	1.13
2 ($\phi = 288.3°$)	2.35	1.53	1.12
2 ($\phi = 318.4°$)	2.39	1.55	1.12
1, 2, and 3 (all ϕ)	2.38 ± 0.03	1.56 ± 0.02	1.12 ± 0.02
2 and 3 (all ϕ)	2.39 ± 0.03	1.56 ± 0.02	1.11 ± 0.02

[a]At 82.3 K, density $\rho = 1.629 \pm 0.001$ g/cm^3 (Ref. 2), and refractive index $n = 1.2681$ and 1.2708 at 6328.2 and 4879.9 Å, respectively (Ref. 19).

TABLE IV. Maximum frequency changes in the acoustic modes resulting from uncertainties of ± 0.5° in the Euler angles (θ, ϕ, χ).

	Frequencies (GHz)			Frequencies (GHz)		
ϕ (deg)	L	T_1	ϕ (deg)	L	T_1	T_2
	Crystal No. 1			Crystal No. 2		
219.3	± 0.008	•••	231.6	± 0.015	± 0.015	± 0.017
229.1	± 0.014	•••	238.3	± 0.010	± 0.019	•••
239.6	± 0.010	•••	249.1	± 0.010	± 0.017	•••
249.3	± 0.013	± 0.016	262.8	± 0.010	± 0.011	•••
259.3	± 0.016	± 0.020	275.4	± 0.015	•••	•••
264.4	± 0.015	± 0.023	288.3	± 0.005	± 0.017	± 0.020
269.9	± 0.015	± 0.022	297.1	± 0.006	± 0.019	•••
274.4	± 0.014	± 0.024	303.9	± 0.006	± 0.015	•••
	Crystal No. 3		306.9	± 0.010	± 0.011	•••
5.0	± 0.014	± 0.022	313.0	± 0.005	± 0.009	•••
16.9	± 0.015	± 0.027	318.4	± 0.010	± 0.012	± 0.011
28.0	± 0.010	± 0.026	321.8	± 0.005	± 0.021	•••
39.0	± 0.005	± 0.021				
53.0	± 0.005	•••				
67.0	± 0.010	± 0.020				
78.1	± 0.015	± 0.027				
91.0	± 0.014	± 0.029				
100.5	± 0.014	± 0.023				

yield a best fit to the combined data for all three crystals. These values were derived using the first method of analysis described above (all ϕ) and are included in Table III. Also shown are values of the elastic constants which give a best fit to the more accurate combined data of crystals 2 and 3.

In order to assess the accuracy of the elastic-constant values determined in the present experiment two types of uncertainty were considered. First, there are uncertainties which affect the absolute magnitude of all three elastic-constant values in the same way, for example, uncertainties in the physical constants of the sample, such as its temperature, density, and refractive index, and uncertainty in the scattering angle. These quantities appear as common factors in the equations used to derive the elastic constants from the Brillouin shifts. The uncertainty in the elastic constants contributed by uncertainties in all four factors combined was estimated to be less than ±1%. Second, there are uncertainties which primarily affect the relative values of the elastic constants, for example, uncertainties in the orientation angles (θ, ϕ, χ), and in the Brillouin shifts. In the present experiment, the maximum uncertainty in each of the Euler angles was estimated to be ±0.5°, and in each of the measured frequency shifts ±1% (Table I).

In order to estimate the effect of these uncertainties on the determination of the elastic constants the following calculation was carried out: For every crystal orientation, the changes in the acoustic-mode frequencies caused by all combinations of $\Delta\theta$, $\Delta\phi$, and $\Delta\chi$ (each equal to ±0.5°) were determined from the dynamical equations. The maximum values of the frequency changes are given in Table IV; these values were added to the corresponding uncertainties in the measured Brillouin shifts given in Table I. The results are indicated by the error bars in Fig. 6. In separate calculations on each crystal, all combinations of C_{11}, C_{12}, and C_{44} which gave a fit to the Brillouin shifts within the error bars were determined from the dynamical equations. In a similar calculation, the combined data of crystals 2 and 3 were fitted. The results of these analyses yielded the errors included with the values of the elastic constants in Table III. A higher accuracy was obtained with crystals 2 and 3 because they were studied over a larger range of orientation angles ϕ (~90° compared to 55° for crystal 1). The best results were achieved with crystal 3 since, in addition, the measured change in frequency shift with orientation angle for the L and T_1 modes was twice the corresponding change observed for crystal 2. Finally, the good agreement between the values of the elastic constants obtained for crystals 2 and 3 indicates that the experimental accuracy is at least as good as given in Table III.

In summary, the experimental data for all three crystals lead to the following values for the adiabatic elastic constants of argon at 82.3 K:

$C_{11} = 2.38 \pm 0.04$,

$C_{12} = 1.56 \pm 0.03$,

$C_{44} = 1.12 \pm 0.03$,

in units of 10^{10} dyn/cm^2.

From these values of the elastic constants, the adiabatic bulk modulus and the elastic anisotropy are found to be

$$B_s = \tfrac{1}{3}(C_{11} + 2C_{12}) = (1.83 \pm 0.03) \times 10^{10} \text{ dyn/cm}^2,$$

$$A = 2C_{44}/(C_{11} - C_{12}) = 2.73 \pm 0.10.$$

The Grüneisen parameter $\gamma = \beta B_s/(\rho C_p)$ is calculated to be 2.77 ± 0.09 at 82.3 K, using the above value of B_s, with the volume expansivity[2] $\beta = (21.24 \pm 0.10) \times 10^{-4}$ K^{-1}, the density[2] $\rho = 1.629 \pm 0.001$ g/cm^3, and the specific heat at constant pressure[20] $C_p = 8.23 \pm 0.07$ cal/mole K.

C. Evaluation of ratios of elasto-optic constants

The intensity ratios $I(T_1)/I(L)$ for crystals 2 and 3 given in Table II, together with values of the elastic constants, scattering geometries, and crystal orientations, were used to determine the ratios p_{12}/p_{11} and p_{44}/p_{11}. Trial values of these ratios were used in Eq. (19)[21] of Ref. 15 to calculate the relative intensities which best fitted the observed intensities. For both crystals, the best agreement (Fig. 7) obtained by least-squares calculations was found for the values,

$$p_{12}/p_{11} = 0.98 \pm 0.16 \quad \text{and} \quad p_{44}/p_{11} = 0.12 \pm 0.05.$$

It must be emphasized that these values are approximate only, since the intensity ratios $I(T_2)/I(L)$ were not included in the evaluation, and moreover, the T_1 component was of very low intensity in the spectra of several crystal orientations. Nevertheless, it may be noted that theory predicts the highest intensities for the T_2 component at just those orientations for which it was observed [Fig. 7(a)].

V. DISCUSSION AND COMPARISON OF PRESENT RESULTS WITH OTHER EXPERIMENTAL VALUES, AND WITH THEORETICAL CALCULATIONS

Summary of the available experimental values of elastic constants of argon is given in Table V. The first determinations of the elastic constants of argon were based on ultrasonic measurements of the velocities of longitudinal and transverse waves propagating in specific crystal directions. Such measurements were made by Moeller and Squire[8] over the temperature range from 74 to 84 K, and by Gsänger, Egger, and Lüscher[9] from 4 to 77 K. The latter combined their data with compressibility measurements[2] in order to obtain values for all three elastic constants. The most recent ultrasonic measurements are those reported by Keeler and Batchelder.[7] In their experiments, argon crystals were grown in an arbitrary orientation around a small transducer suspended in a Mylar sample cell. Velocities of longitudinal and transverse ultrasonic waves were measured by the pulse-echo technique. Both the transducer mounting and the cell wall were flexible, so that the crystal was apparently not damaged as the temperature was changed from 77 to 3 K. The crystal size, quality, and orientation were determined by back reflection of x rays. However, the authors have noted that the crystal structure in their samples could not be determined at the crystal-transducer and crystal-substrate interfaces.

The results of these three ultrasonic experiments are summarized in Table V. A comparison of corresponding values at similar temperatures, for example, at 4 and 4.2 K, and at 82, 76.8, and 80 K, shows widely differing values among the three sets of ultrasonic data. Furthermore, there is significant disagreement between any set of ultra-

TABLE V. Summary of experimental values of adiabatic elastic constants and of elastic anisotropy A, for argon.

Experiment	Temp. (K)	C_{11} (10^{10} dyn/cm^2)	C_{12} (10^{10} dyn/cm^2)	C_{44} (10^{10} dyn/cm^2)	A
Brillouin scattering					
Present results	82.3	2.38	1.56	1.12	2.73 ± 0.10
Ultrasonic measurements					
Moeller and Squire, Ref. 8	82	2.81	1.57	0.56	0.90
Gsänger *et al.*, Ref. 9	4.2	5.29	1.35	1.59	0.81 ± 0.21
	76.8	3.35	1.01	0.93	0.80 ± 0.28
Keeler and Batchelder, Ref. 7	4	4.38	1.82	1.63	1.27 ± 0.18
	40	3.77	1.77	1.35	1.35 ± 0.20
	80	2.70	1.39	0.89	1.36 ± 0.23
Neutron scattering					
Batchelder *et al.* Ref. 10	4	4.11	1.90	2.10	1.90
Egger *et al.*, Ref. 11	4.2	3.67	1.74	2.34	2.42 ± 0.30
Stimulated Brillouin scattering					
Meixner *et al.*, Ref. 24	80	2.77	1.16	1.12	1.39

sonic values at ~80 K and those obtained in the present experiment at 82.3 K. It should also be pointed out that all of the ultrasonic data lead to values of the elastic anisotropy A between 0.8 and 1.4, a result which may be inferred to arise from polycrystalline samples rather than from single crystals. These values for A are almost half the value obtained in the present experiment.

The elastic constants of solid argon have also been measured by neutron scattering experiments, although only at 4 K. In these experiments, phonon dispersion curves of the crystal are measured, and a fit to the experimental curves yields a set of interatomic force constants, which in turn are used to derive values of the elastic constants. The neutron scattering data of Batchelder *et al.*[10] measured from a single crystal of argon at 4 K were analyzed in this way and the elastic constants are given in Table V. In another experiment on argon single crystals at 4.2 K, Egger *et al.*[11] derived the elastic constants from the slopes of the phonon dispersion curves at low frequencies.

The neutron scattering results at 4 K, of course, are not directly comparable to the present values at 82.3 K because of anharmonicity. However, theory predicts that the elastic anisotropy parameter A does not change significantly with temperature. Therefore, it is interesting to note that the values of A determined from neutron scattering data are closer to the present experimental value than were the ultrasonic values. It should also be pointed out that values of the elastic constants obtained by neutron scattering and by ultrasonic measurements or Brillouin scattering, at the same temperature, may not be identical because of possible dispersion. For example, calculations by Niklasson[22] on argon at its triple point suggest differences of ~4%, and recent measurements[23] on krypton near its triple point indicate differences as large as 10%.

Another technique used recently in the determination of sound velocities is stimulated Brillouin scattering. Meixner *et al.*[24] have reported longitudinal sound-velocity measurements for propagation in the [100] and [110] directions in single crystals of argon, over the temperature range 4.2 to 77 K. The elastic constant C_{11} was determined directly from the velocity in the [100] direction, and values of C_{12} and C_{44} were obtained by combining the data in the [110] direction with compressibility measurements on argon.[2] The results show a smooth temperature dependence from 4 to 77 K, and it is straightforward to make a slight extrapolation to obtain the constants at 80 K which are given in Table V. The value of C_{11} at 80 K is approximately 15% larger than the present experimental value. This discrepancy is not understood.

Theoretical values of the adiabatic elastic constants of argon from 0 to 80 K are summarized in Table VI and Fig. 8.

In the conventional treatment of vibrational anharmonicity in lattice dynamics, the crystal potentail energy is expanded to fourth order in the atomic displacements. The cubic and quartic terms are regarded as small fractions of the total potential energy and are handled by perturbation theory (PT). This approach was taken by Feldman, Klein, and Horton[25] in a calculation of the adiabatic elastic constants of argon based on a Lennard-Jones (LJ) (6-12) potential and restricted to nearest-neighbor (NN) interactions. Their results are shown by the dashed curves in Fig. 8. At 0 K, their values are consistent with the quasiharmonic calculation of Barron and Klein.[26] For temperatures greater than approximately one-third of the triple-point temperature, the large ($\gtrsim 6\%$) rms amplitudes of lattice vibrations preclude the suitability of the perturbation-theory approach, and therefore, the computed curves terminate at ~60 K.

The self-consistent phonon theory (SC) provides a more adequate treatment of large-amplitude lattice vibrations. With this approach, much better agreement between theoretical and experimental values of thermodynamic properties of rare-gas solids has been obtained at high temperatures.[27] Klein, Horton, and Goldman[28] have calculated the isothermal elastic constants of argon as functions of temperature using the SC theory with a Lennard-Jones (6-12) potential acting between nearest-neighbors only. Adiabatic isothermal corrections[26] were calculated using the experimental values of Peterson *et al.*[2] for the density, expansivity, and adiabatic bulk modulus together with the specific-heat values of Flubacher *et al.*[20] These corrections were applied to the isothermal elastic constants of Klein *et al.*[28]; the resulting values are shown by the dash-dotted curves in Fig. 8, and included in Table VI. The present experimental value of C_{44} is in good agreement with the SC value. However, the experimental and theoretical values of C_{11} and C_{12} differ by 12 and 11%, respectively.

The SC theory used by Klein *et al.*[28] did not include odd derivatives of the interatomic potential. When they are included (leading to the "improved self-consistent" theory, ISC), the calculated values of the volume expansivity and heat capacity are in better agreement with experimental results, although the bulk-modulus values calculated from the SC and ISC schemes differ by only a few percent.[28] It is unlikely, therefore, that the elastic constants evaluated by the ISC scheme will differ substantially from the SC estimates.

Recently, Monte Carlo (MC) computer methods have been used to evaluate thermodynamic and elastic properties of rare-gas crystals. Since these calculations take all interactions into account

TABLE VI. Theoretical values of adiabatic elastic constants and elastic anisotropy A for argon.

	Potential	Temp. (K)	C_{11}	C_{12} (10^{10} dyn/cm^2)	C_{44}	A
Barron and Klein,	LJ (6-12) (NN)	0	3.98	1.92	2.01	1.95
Ref. 26	(AN)	0	3.71	2.07	2.15	2.62
Feldman *et al.*,	LJ (6-12) (NN)	7	3.97	1.92	2.00	1.95
Ref. 25		59	2.94	1.59	1.22	1.82
Klein *et al.*,	LJ (6-12) (NN)	25	3.81	1.87	1.88	1.92
Ref. 28		83	2.66	1.39	1.15	1.81
Hoover *et al.*,	LJ (6-12) (AN)	40	3.16	1.93	1.69	2.75
Ref. 29		60	2.73	1.76	1.44	2.97
Fisher and Watts,	BFW and ATM (AN)	40	3.60	2.21	1.83	2.62
Ref. 12		60	3.14	1.98	1.54	2.66
		80	2.48	1.65	1.12	2.70
Klein and Murphy, Ref. 13	BB and ATM (AN)	80	2.50	1.62	1.18	2.70
Gibbons *et al.*, Ref. 14	PSL and ATM (AN)	80	2.37	1.57	1.12	2.80
Present results		82.3	2.38	1.56	1.12	2.73

exactly (within the assumptions of a given force law), they are equivalent to theoretical treatments which include all-neighbor interactions (AN). The adiabatic elastic constants of argon have been evaluated at several temperatures by Hoover, Holt, and Squire[29] using a system of 108 particles interacting with a Lennard-Jones (6-12) potential. Their results, given in Table VI, are shown by the open squares in Fig. 8. The Monte Carlo value of C_{11} is lower than that observed experimentally by ~7% although there is excellent agreement for C_{12} and C_{44}. The fact that the AN Monte Carlo results give better agreement with the present experimental values than the NN SC results is an indication that interactions beyond the range of nearest neighbors must be considered.

In all of the theoretical work summarized above, the interaction between atoms was taken to be the familiar Lennard-Jones (6-12) potential. However, it has been recognized for some time that this potential does not give a satisfactory description of dilute-gas properties.[30] Indeed, recent investigations of the absorption spectrum of diatomic argon in the 780–1080-Å region by Tanaka and Yoshino,[4] and measurements of differential scattering cross sections for Ar+Ar in molecular-beam experiments by Scoles[5] and Lee[3] and their co-workers, have confirmed that the Lennard-Jones (6-12) potential does not describe adequately the pair interactions in gaseous argon. Barker[6] and Lee[3] and their colleagues have proposed multiparameter pair potentials which are in good agreement with the spectroscopic and molecular-beam data.

Recent calculations of the elastic constants of argon have been based on the Barker and Pompe (BP) potential

$$\phi_{BP}(k,\ l)=\epsilon\left[\sum_{i=0}^{3}A_i(r-1)^i e^{\alpha(1-r)}-\sum_{j=0}^{2}\frac{C_{2j+6}}{\delta+r^{2j+6}}\right].$$

Here $r=R_{kl}/R_m$, where R_{kl} is the actual separation

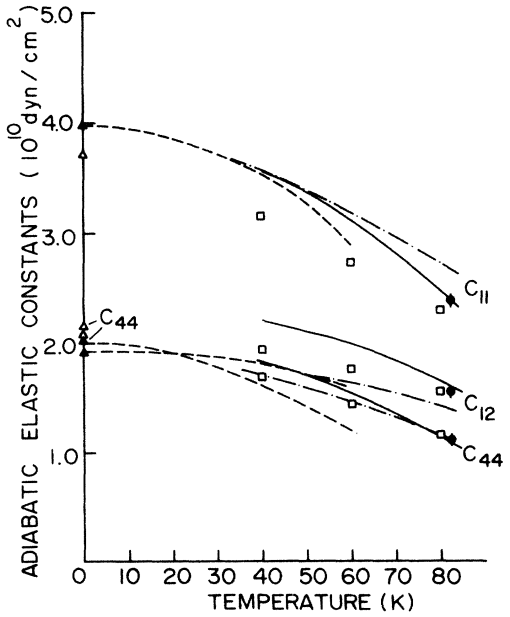

FIG. 8. Adiabatic elastic constants of solid argon as a function of temperatue. The present experimental values are plotted as solid dots. The values at 0 K are the quasiharmonic calculations of Barron and Klein (Ref. 26) for NN (▲) and AN (Δ) interactions. Results of other theoretical calculations are labeled as follows: dashed line, Feldman *et al.* (Ref. 25) (PT); dash-dot line, Klein *et al.* (Ref. 28) (SC); □, Hoover *et al.* (Ref. 29) (MC); solid line, Fisher and Watts (Ref. 12) (MC).

of the atoms k and l, and R_m denotes the separation, and ϵ the depth, at the minimum of the potential. The many parameters were evaluated, in part, from fitting to thermodynamic and transport properties of dilute gaseous argon. In order to obtain good agreement with experimental data for condensed argon using this pair potential, it was necessary to include the Axilrod-Teller-Muto (ATM) triple-dipole interaction given by[31]

$$\phi_{\mathrm{ATM}}(klm) = \nu \frac{1 + 3\cos\theta_k \cos\theta_l \cos\theta_m}{(R_{kl} R_{lm} R_{mk})^3} .$$

Here R_{kl}, R_{lm}, R_{mk} and θ_k, θ_l, θ_m are the sides and angles, respectively, of the triangle formed by the atoms k, l, and m, and ν is a constant which is evaluated theoretically.[13] Bobetic and Barker[6] (BB) have refined the BP pair potential by imposing a fit to properties of solid argon at 0 K. In a further refinement, Barker, Fisher, and Watts[6] (BFW) have used a linear combination of the BP and BB pair potentials, namely,

$$\phi_{\mathrm{BFW}}(k, l) = 0.75\phi_{\mathrm{BB}}(k, l) + 0.25\phi_{\mathrm{BP}}(k, l),$$

and have obtained good agreement with experimental data on gaseous, liquid, and solid-state properties of argon.

Fisher and Watts[12] have used the BFW pair potential together with the ATM potential in a Monte Carlo calculation of the adiabatic elastic constants of argon as functions of the temperature. Their results are given in Table VI and shown in Fig. 8 by the solid curves. The agreement with the present experimental values at 82.3 K is excellent for all three elastic constants. Klein and Murphy[13] have used the BB and ATM potentials in a similar Monte Carlo calculation and have obtained the adiabatic elastic constants at 80 K. It can be seen that their results, given in Table VI, are very similar to the values obtained by Fisher and Watts.[12] Finally, Gibbons, Klein, and Murphy[14] have used the pair potential of Parson, Siska, and Lee[3] (PSL) with the ATM potential in a Monte Carlo calculation at 80 K. Their elastic-constant values are comparable to the results obtained with the BFW[12] and BB[13] pair potentials.

In all three Monte Carlo calculations summarized above, the contribution of the ATM triple-dipole interaction to the adiabatic elastic constants is approximately $+0.2\times10^{10}$ dyn/cm^2 for C_{11} and C_{12} and zero for C_{44}.[14] It should be noted that the triple-dipole contributions are larger than the errors in the present experimental results. Although the ATM contributions are small, nevertheless, the excellent agreement between the theoretical and the present experimental values suggests that the pair potentials of Barker and his co-workers and of Parson, Siska, and Lee are good representations of the pair interactions between argon atoms in the solid. Furthermore, it appears necessary to include many-body interactions in theoretical calculations of the elastic properties of solid argon, and the ATM triple-dipole interaction may be a useful approximation to these many-body forces.

When the elastic-constant values obtained from the ultrasonic and neutron scattering experiments were compared with each of the theoretical calculations discussed above, a serious disagreement was found in the value of at least one elastic constant of each set. More striking was the disagreement with the theoretical values for the elastic anisotropy parameter A given in Table VI. By contrast, the present experimental value of $A = 2.73 \pm 0.10$ is in good agreement with that predicted by the recent theoretical calculations.

VI. CONCLUSIONS

The adiabatic elastic constants of argon single crystals were determined to an accuracy of better than 2.5% by high-resolution Brillouin spectroscopy. The present experimental values differ significantly from the values obtained in earlier investigations based on neutron scattering and ultrasonic measurements. However, in contrast to this earlier work, the strength of the present method lies in the knowledge that measurements were carried out on single crystals.

The present experimental values of the elastic constants and the elastic anisotropy show good agreement with recent Monte Carlo calculations. The good agreement with the results of such calculations based on the Lennard-Jones (6-12) potential is somewhat surprising, since recent molecular-beam and spectroscopic results have definitely ruled out this potential for gaseous argon. Alternative pair potentials have been developed which are consistent with this recent data on Ar_2 molecules. The elastic constants and elastic anisotropy calculated by the Monte Carlo method using these pair potentials do not agree with the present experimental values if pairwise additivity of the interatomic potentials is assumed. However, if the nonadditivity is approximated by the Axilrod-Teller-Muto triple-dipole interaction, these Monte Carlo calculations show excellent agreement with the present experimental values. This reinforces current theoretical opinion that many-body forces contribute to the properties of condensed argon.

The present experiment has yielded much useful data; however, the measurements were made at one temperature only, just below the triple point. Clearly, further experimental measurements of the elastic constants of argon at lower temperatures would be desirable. It would also be of value to make measurements of the absolute intensity of the Brillouin scattering in order to derive absolute values of the elasto-optic coefficients.

ACKNOWLEDGMENTS

We are grateful to M. L. Klein for helpful discussions on the theory, to R. A. McLaren and D. Landheer, for assistance with the computer programme, and to W. S. Gornall and A. Jares for advice on experimental problems.

---

*Research supported in part by the National Research Council of Canada and the University of Toronto. The work reported here is based on the thesis by S. Gewurtz submitted for the Ph. D. degree to the University of Toronto in 1973. Brief preliminary reports of this work have been presented at a meeting of the Canadian Association of Physicists [Phys. Can. 28, 13 (1972)] and in Ref. 16.

†Holder of a National Research Council of Canada Scholarship 1967–1970, and an E. F. Burton Scholarship, University of Toronto 1971. Present address: Physics Division, National Research Council of Canada, Ottawa, Ontario K1A OR6.

[1]O. G. Peterson, D. N. Batchelder, and R. O. Simmons, J. Appl. Phys. 36, 2682 (1965); D. N. Batchelder, D. L. Losee, and R. O. Simmons, in *Crystal Growth*, edited by H. S. Peiser (Pergamon, New York, 1967), p. 843.

[2]O. G. Peterson, D. N. Batchelder, and R. O. Simmons, Phys. Rev. 150, 703 (1966); A. O. Urvas, D. L. Losee, and R. O. Simmons, J. Phys. Chem. Solids 28, 2269 (1967).

[3]J. M. Parson, P. E. Siska, and Y. T. Lee, J. Chem. Phys. 56, 1511 (1972).

[4]Y. Tanaka and K. Yoshino, J. Chem. Phys. 53, 2012 (1970).

[5]M. Cavallini, G. Gallinaro, L. Meneghetti, G. Scoles, and U. Valbusa, Chem. Phys. Lett. 7, 303 (1970).

[6]J. A. Barker and A. Pompe, Aust. J. Chem. 21, 1683 (1968); M. V. Bobetic and J. A. Barker, Phys. Rev. B 2, 4169 (1970); J. A. Barker, R. A. Fisher and, R. O. Watt, Mol. Phys. 21, 657 (1971).

[7]G. J. Keeler and D. N. Batchelder, J. Phys. C 3, 510 (1970).

[8]H. R. Moeller and C. F. Squire, Phys. Rev. 151, 689 (1966).

[9]M. Gsänger, H. Egger, and E. Lüscher, Phys. Lett. A 27, 695 (1968).

[10]D. N. Batchelder, M. F. Collins, B. C. G. Haywood, and G. R. Sidey, J. Phys. C 3, 249 (1970).

[11]H. Egger, M. Gsänger, E. Lüscher, and B. Dorner, Phys. Lett. A 28, 433 (1968); B. Dorner and H. Egger, Phys. Status Solidi B 43, 611 (1971).

[12]R. A. Fisher and R. O. Watts, Mol. Phys. 23, 1051 (1972).

[13]M. L. Klein and R. D. Murphy, Phys. Rev. B 6, 2433 (1972).

[14]T. G. Gibbons, M. L. Klein, and R. D. Murphy (unpublished).

[15]W. S. Gornall and B. P. Stoicheff, Solid State Commun. 8, 1529 (1970); Phys. Rev. B 4, 4518 (1971).

[16]S. Gewurtz, H. Kiefte, D. Landheer, R. A. McLaren, and B. P. Stoicheff, Phys. Rev. Lett. 29, 1454; 29, 1768(E) (1972).

[17]G. B. Benedek and K. Fritsch, Phys. Rev. 149, 647 (1966).

[18]P. W. Smith, IEEE J. Quantum Electron. QE-1, 343 (1965); QE-2, 666 (1966).

[19]A. C. Sinnock and B. L. Smith, Phys. Rev. 181, 1297 (1969).

[20]P. Flubacher, A. J. Leadbetter, and J. A. Morrison, Proc. Phys. Soc. Lond. A 78, 1449 (1961).

[21]Equation (19) perpetuates an earlier error in which p_{44} is taken to be twice the value of the conventional definition. See N. R. Werthamer, Phys. Rev. B 6, 4075 (1972).

[22]G. Niklasson, Phys. Kondens. Mater. 14, 138 (1972).

[23]H. E. Jackson, D. Landheer, and B. P. Stoicheff, Phys. Rev. Lett. 31, 296 (1973).

[24]H. Meixner, P. Leiderer, P. Berkerich, and E. Lüscher, Phys. Lett. A 37, 39 (1971); 40, 257 (1972).

[25]C. Feldman, M. L. Klein, and G. K. Horton, Phys. Rev. 184, 910 (1969).

[26]T. H. K. Barron and M. L. Klein, Proc. Phys. Soc. Lond. 85, 533 (1965).

[27]V. V. Goldman, G. K. Horton, and M. L. Klein, Phys. Rev. Lett. 21, 1527 (1968); Phys. Lett. A 28, 341 (1968); M. L. Klein, V. V. Goldman, and G. K. Horton, J. Phys. Chem. Solids 31, 2441 (1970).

[28]M. L. Klein, G. K. Horton, and V. V. Goldman, Phys. Rev. B 2, 4995 (1970).

[29]W. G. Hoover, A. C. Holt, and D. R. Squire, Physica 44, 437 (1969); 42, 388 (1969).

[30]E. A. Guggenheim and M. L. McGlashan, Proc. R. Soc. A 255, 456 (1960).

[31]B. M. Axilrod and E. Teller, J. Chem. Phys. 11, 299 (1943); B. M. Axilrod, J. Chem. Phys. 19, 719 (1951); W. Götze and H. Schmidt, Z. Phys. 192, 409 (1966).

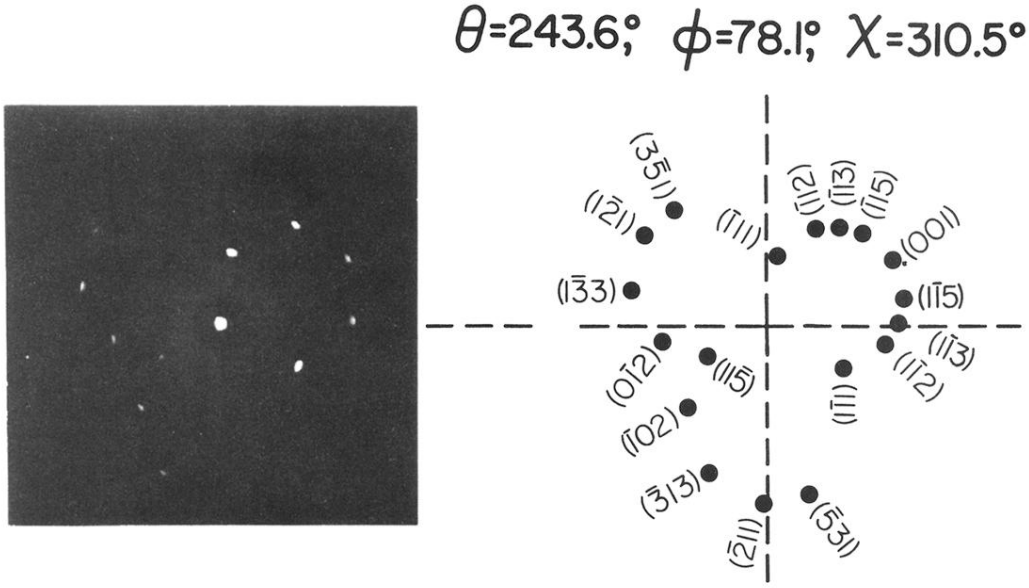

FIG. 3. Photograph of Laue diffraction pattern of crystal 3 ($\theta = 243.6°$, $\phi = 78.1°$, $\chi = 310.5°$) and the computed pattern which identified the crystal orientation. The solid circles in the computed pattern correspond to the observed diffraction spots.